

## Progress in the realization of the PRIMA neutral beam test facility

This content has been downloaded from IOPscience. Please scroll down to see the full text.

2015 Nucl. Fusion 55 083025

(<http://iopscience.iop.org/0029-5515/55/8/083025>)

View [the table of contents for this issue](#), or go to the [journal homepage](#) for more

Download details:

IP Address: 150.178.3.9

This content was downloaded on 30/07/2015 at 13:15

Please note that [terms and conditions apply](#).

# Progress in the realization of the PRIMA neutral beam test facility

V. Toigo<sup>1</sup>, D. Boilson<sup>2</sup>, T. Bonicelli<sup>3</sup>, R. Piovan<sup>1</sup>, M. Hanada<sup>4</sup>,  
A. Chakraborty<sup>5</sup>, G. Agarici<sup>3</sup>, V. Antoni<sup>1</sup>, U. Baruah<sup>5</sup>, M. Bigi<sup>1</sup>, G. Chitarin<sup>1</sup>,  
S. Dal Bello<sup>1</sup>, H. Decamps<sup>2</sup>, J. Graceffa<sup>2</sup>, M. Kashiwagi<sup>4</sup>, R. Hemsworth<sup>2</sup>,  
A. Luchetta<sup>1</sup>, D. Marcuzzi<sup>1</sup>, A. Masiello<sup>3</sup>, F. Paolucci<sup>3</sup>, R. Pasqualotto<sup>1</sup>,  
H. Patel<sup>5</sup>, N. Pomaro<sup>1</sup>, C. Rotti<sup>5</sup>, G. Serianni<sup>1</sup>, M. Simon<sup>3</sup>, M. Singh<sup>2</sup>,  
N.P. Singh<sup>5</sup>, L. Svensson<sup>2</sup>, H. Tobar<sup>4</sup>, K. Watanabe<sup>4</sup>, P. Zaccaria<sup>1</sup>,  
P. Agostinetti<sup>1</sup>, M. Agostini<sup>1</sup>, R. Andreani<sup>1</sup>, D. Aprile<sup>1</sup>, M. Bandyopadhyay<sup>5</sup>,  
M. Barbisan<sup>1</sup>, M. Battistella<sup>1</sup>, P. Bettini<sup>1</sup>, P. Blatchford<sup>7</sup>, M. Boldrin<sup>1</sup>,  
F. Bonomo<sup>1</sup>, E. Bragulat<sup>3</sup>, M. Brombin<sup>1</sup>, M. Cavenago<sup>12</sup>, B. Chuilon<sup>7</sup>,  
A. Coniglio<sup>15</sup>, G. Croci<sup>10</sup>, M. Dalla Palma<sup>1</sup>, M. D'Arienzo<sup>13</sup>, R. Dave<sup>5</sup>,  
H. P. L. De Esch<sup>9</sup>, A. De Lorenzi<sup>1</sup>, M. De Muri<sup>1</sup>, R. Delogu<sup>1</sup>, H. Dhola<sup>5</sup>,  
U. Fantz<sup>6</sup>, F. Fellin<sup>1</sup>, L. Fellin<sup>1</sup>, A. Ferro<sup>1</sup>, A. Fiorentin<sup>1</sup>, N. Fomesu<sup>1</sup>,  
P. Franzen<sup>6</sup>, M. Fröschele<sup>6</sup>, E. Gaio<sup>1</sup>, G. Gambetta<sup>1</sup>, G. Gomez<sup>3</sup>, F. Gnesotto<sup>1</sup>,  
G. Gorini<sup>11</sup>, L. Grandi<sup>1</sup>, V. Gupta<sup>5</sup>, D. Gutierrez<sup>3</sup>, S. Hanke<sup>8,9</sup>, C. Hardie<sup>7</sup>,  
B. Heinemann<sup>6</sup>, A. Kojima<sup>4</sup>, W. Kraus<sup>6</sup>, T. Maeshima<sup>4</sup>, A. Maistrello<sup>1</sup>,  
G. Manduchi<sup>1</sup>, N. Marconato<sup>1</sup>, G. Mico<sup>3</sup>, J. F. Moreno<sup>3</sup>, M. Moresco<sup>1</sup>,  
A. Muraro<sup>1</sup>, V. Muvvala<sup>5</sup>, R. Nocentini<sup>6</sup>, E. Ocello<sup>1</sup>, S. Ochoa<sup>8,9</sup>, D. Parmar<sup>5</sup>,  
A. Patel<sup>5</sup>, M. Pavei<sup>1</sup>, S. Peruzzo<sup>1</sup>, N. Pilan<sup>1</sup>, V. Pilard<sup>3</sup>, M. Recchia<sup>1</sup>, R. Riedl<sup>6</sup>,  
A. Rizzolo<sup>1</sup>, G. Roopesh<sup>5</sup>, G. Rostagni<sup>1</sup>, S. Sandri<sup>14</sup>, E. Sartori<sup>1</sup>, P. Sonato<sup>1</sup>,  
A. Sottocornola<sup>1</sup>, S. Spagnolo<sup>1</sup>, M. Spolaore<sup>1</sup>, C. Taliercio<sup>1</sup>, M. Tardocchi<sup>10</sup>,  
A. Thakkar<sup>5</sup>, N. Umeda<sup>4</sup>, M. Valente<sup>1</sup>, P. Veltri<sup>1</sup>, A. Yadav<sup>5</sup>, H. Yamanaka<sup>4</sup>,  
A. Zamengo<sup>1</sup>, B. Zaniol<sup>1</sup>, L. Zanotto<sup>1</sup> and M. Zaupa<sup>1</sup>

<sup>1</sup> Consorzio RFX, Corso Stati Uniti 4, 35127 Padova, Italy

<sup>2</sup> ITER Organization, Route de Vinon sur Verdon, CS 90 046, 13067 St. Paul Lez Durance Cedex, France

<sup>3</sup> Fusion For Energy, C/ Josep Pla 2, 08019 Barcelona, Spain

<sup>4</sup> Japan Atomic Energy Agency, 801-1 Mukoyama, Naka, Ibaraki-ken 311-0193, Japan

<sup>5</sup> Institute for Plasma Research, Nr. Indira Bridge, Bhat Village, Gandhinagar, Gujarat 382428, India

<sup>6</sup> IPP, Max-Planck Institut für Plasmaphysik, D-85748 Garching, Germany

<sup>7</sup> CCFE, Culham Science Centre, Oxfordshire, UK

<sup>8</sup> KIT, Institute for Technical Physics, Eggenstein-Leopoldshafen, Germany

<sup>9</sup> CEA-Cadarache, IRFM, F-13108 Saint-Paul-lez-Durance, France

<sup>10</sup> Istituto di Fisica del Plasma 'P. Caldirola', Milano, Italy

<sup>11</sup> Dipartimento di Fisica 'G. Occhialini', Università di Milano-Bicocca, Milano, Italy

<sup>12</sup> INFN-LNL, viale dell'Università n. 2, 35020 Legnaro, Italy

<sup>13</sup> ENEA, National Institute of Ionizing Radiation Metrology, C.R. Casaccia, S.Maria di Galeria, Italy

<sup>14</sup> ENEA Radiation Protection Institute, Frascati (Roma), Italy

<sup>15</sup> Ospedale Fatebenefratelli-Isola Tiberina, Roma, Italy

E-mail: [vanni.toigo@igi.cnr.it](mailto:vanni.toigo@igi.cnr.it)

Received 23 January 2015, revised 4 May 2015

Accepted for publication 16 June 2015

Published 21 July 2015



CrossMark

## Abstract

The ITER project requires additional heating by two neutral beam injectors, each accelerating to 1 MV a 40 A beam of negative deuterium ions, to deliver to the plasma a power of about 17 MW for one hour. As these requirements have never been experimentally met, it was

recognized as necessary to setup a test facility, PRIMA (Padova Research on ITER Megavolt Accelerator), in Italy, including a full-size negative ion source, SPIDER, and a prototype of the whole ITER injector, MITICA, aiming to develop the heating injectors to be installed in ITER. This realization is made with the main contribution of the European Union, through the Joint Undertaking for ITER (F4E), the ITER Organization and Consorzio RFX which hosts the Test Facility. The Japanese and the Indian ITER Domestic Agencies (JADA and INDA) participate in the PRIMA enterprise; European laboratories, such as IPP-Garching, KIT-Karlsruhe, CCFE-Culham, CEA-Cadarache and others are also cooperating. Presently, the assembly of SPIDER is on-going and the MITICA design is being completed. The paper gives a general overview of the test facility and of the status of development of the MITICA and SPIDER main components at this important stage of the overall development; then it focuses on the latest and most critical issues, regarding both physics and technology, describing the identified solutions.

Keywords: ITER, negative neutral beam, PRIMA test facility, RF ion source, 1 MV acceleration voltage

(Some figures may appear in colour only in the online journal)

## 1. Introduction

In ITER, additional heating systems are required to allow the L-H transition, to reach high plasma temperature and to sustain fusion conditions; among them two neutral beam injectors (NBI) will be installed, capable of producing high energy beams up to 1 MeV; they will be based on the neutralisation of electrostatically-accelerated negative ions, will transfer to the plasma up to about 17 MW each and will operate up to 1 h [1, 2].

The required acceleration energy, negative ion current density and stationary conditions have never been obtained simultaneously, even if some of them have already been reached separately in present NBI systems and test facilities: extracted current density and pulse duration of the RF sources at IPP-Garching [3, 4]; parameters of the full beam lines in the Japanese facilities at JAEA [5] and NIFS [6] where also the 1 MeV particle energy has been achieved [7]. A research and development plan has been launched to minimize the risks of unsuccessful results of the ITER NBI operation [8, 9]; it includes the realization of a full scale test facility in which issues related to NBI physics and technology like negative ion yield, current uniformity, 1 MV voltage holding, beam transport and neutralization, operation of beam line components and power supplies, overall reliability of the injector, will be studied and assessed in advance of the ITER operation to guarantee the achievement of the full ITER performance [10]. This test facility, called PRIMA (Padova Research on ITER Megavolt Accelerator), is under construction in Padova, Italy. It will host two experiments: MITICA and SPIDER, full scale prototypes of the whole injector and of the ion source, respectively [11]. PRIMA provides the experimental devices with the necessary auxiliary systems. MITICA (Megavolt ITER Injector and Concept Advancement) [12] is the full-scale prototype of the ITER injector, with a similar scheme, layout and power supplies. The control and protection systems are being designed according to the rules and constraints defined for the integration of ITER plant systems. Only the auxiliary systems, e.g. cooling, cryogenic, vacuum and gas,

SF<sub>6</sub> plants are specifically designed for the facility, with the performance required to satisfy the operation at full power. MITICA will aim to study the whole injector operation, including the beam acceleration, focalization and neutralization. The present design is the result of the existing knowledge on NBIs gained in the past and of the R and D work carried out in the last decade which allowed solving some preliminary fundamental issues. SPIDER (source for production of ion of deuterium extracted from Rf plasma) [13] will be a radiofrequency (RF) ion source, based on the configuration developed by IPP [14], with the same characteristics foreseen for the ITER NBI but with beam energy limited to 100 keV. It can generate both Hydrogen and Deuterium negative ions using caesium to attain the high values of current density required in the ITER NB ion source. Downstream of the accelerator an electron dump filters the co-extracted electrons. SPIDER mission is to increase the understanding of source operation and to optimize the source performance. This will also be done in close collaboration with IPP-Garching, where the ELISE device [15] has started operation in 2013. ELISE is half the size of SPIDER and has been constructed within the European roadmap [16] towards the realization of the ITER NBI. SPIDER and MITICA will allow carrying out an experimental program dedicated to addressing the physics and technological issues of the ITER NBI, reaching the target performance, improving the reliability of the NBI operation and verifying the validity and robustness of the adopted design solutions. Concerning this final topic, possible modifications or upgrade of some parts can be considered and realized in view of an optimization of the final system for ITER.

## 2. General overview of the test facility

### 2.1. PRIMA

PRIMA premises, see figure 1, involves a total area of 17 500 m<sup>2</sup>, of which 7,400 m<sup>2</sup> are covered, and a total volume of about 150 000 m<sup>3</sup>. The maximum height of the building,



**Figure 1.** PRIMA site hosting SPIDER and MITICA experiments.

where the injectors are hosted, is about 24 m. SPIDER and MITICA experiments are hosted in the main building and are individually shielded by concrete barriers for deuterium operation having a thickness of 1.2 m and 1.8 m respectively. This allows safe access to the area, even during the operation of either experiment. Further buildings are dedicated to accommodate power supplies, auxiliaries and common plant systems, control systems, protection and diagnostics. An important requirement for the building layout was dictated by the need to maintain the MITICA layout as close as possible to the one of the ITER heating neutral beam injector (HNB).

Three auxiliary plant systems are common to the two experiments: a) 22 kV medium voltage distribution system. The electrical power required by each experiment, 15 MVA for SPIDER and 76 MVA by MITICA, are taken from the 400 kV Italian national grid via two 50 MVA step down transformers. The power is distributed to each experiment via a dedicated 22 kV medium voltage distribution system. Each experiment will be provided with its own medium voltage Distribution Board. Sufficient power is available to operate the two experiments simultaneously. b) Cooling system: it is sized to dissipate in the environment around 70 MW of power absorbed from the experiments and related auxiliary facilities. In order to reduce the rating of the cooling towers, the heat produced during the operation of the experiments will be stored in the water contained in two underground water basins and exhausted to the environment by cooling towers during the interval in between two beam pulses. Taking into account that the maximum duty cycle is 1/4, the cooling towers are sized for approximately 17 MW. Design and procurement progress of the cooling system is described in [17]. c) Gas and vacuum injection system: it includes a common segment of gas storage and distribution system and two independent vacuum and gas injection systems dedicated to the SPIDER and MITICA experiments respectively. Design and procurement progress of the gas and vacuum injection system is described in [12].

## 2.2. MITICA

MITICA is a full scale prototype of the ITER neutral beam injector, see figure 2, identical to the ITER HNB, including the power supply system and HV transmission line, see figure 3.

The MITICA beam source, shown in figure 4 is the most complex part of the injector; it includes a RF-driven ion

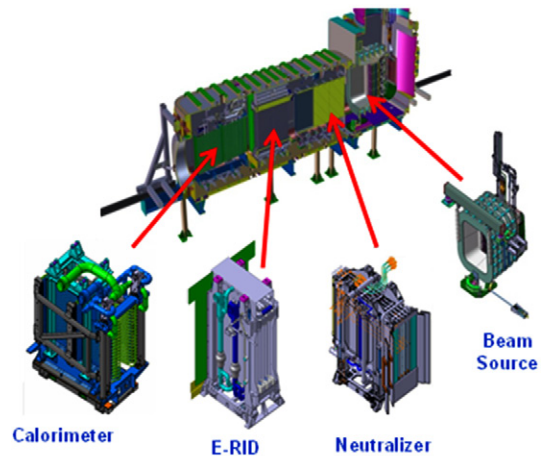


**Figure 2.** Section of MITICA Injector with view of the internal components.

source, similar to the SPIDER one, and the accelerator. The RF ion source, placed in the rear part of the beam source, is devoted to the production of negative ions, operating with 0.3 Pa hydrogen or deuterium gas. A series of conductive grids ( $1600 \times 600 \text{ mm}^2$  size, 10–17 mm thickness and 1280 apertures), kept at different electric potentials, constitute the ion extractor and electrostatic accelerator and produce a negative ion beam of 46 A  $\text{H}^-$  (or a 40 A  $\text{D}^-$ ) formed by 1280 individual beamlets. The negative ions available in the plasma source (where a negative electric potential of about 1000 kV is applied for operation with  $\text{D}_2$  and 870 kV for operation with  $\text{H}_2$ ) are extracted across the gap between the plasma grid (PG) and the extraction grid (EG) and accelerated toward the grounded grid (GG). Four additional acceleration grids (AG1–AG4) at intermediate electric potential, located between the EG and the GG, constitute a 5-stage electrostatic accelerator.

The resulting negative ion beam at 1 MeV  $\text{D}^-$  or 870 keV  $\text{H}^-$ , after passing through a gas-cell neutralizer and electron dump (NED) and the electrostatic residual ion dump (E-RID), produces a  $\sim 17$  MW Neutral Beam which will be intercepted by a target Calorimeter for a duration up to 3600 s [18, 19]. All components of the MITICA injector will be contained in a vacuum vessel, made of stainless steel AISI 304L, that is composed of two parts, the beam line vessel (BLV) and the beam source vessel (BSV), welded together on site for transportation reasons. Several cooling water circuits are foreseen to actively cool the Beam Source, removing a total power of 10 MW and guaranteeing an accurate control of temperatures during the pulse operation.

The neutralizer [20], whose aim is to neutralize the high energy ions by charge exchange with gas molecules of the same type, is composed of 4 channels with the lateral walls being water cooled copper panels which receive a total power of up to 5 MW.  $\text{D}_2$  or  $\text{H}_2$  is injected midway along each neutraliser channel. The neutralization efficiency of the high energy negative beam is about 60%, so a significant amount of positive and negative ions have to be filtered downstream of the neutralizer. This function is performed by the E-RID by applying a transverse electric field. Similarly to the neutralizer, the E-RID is composed of five longitudinal panels

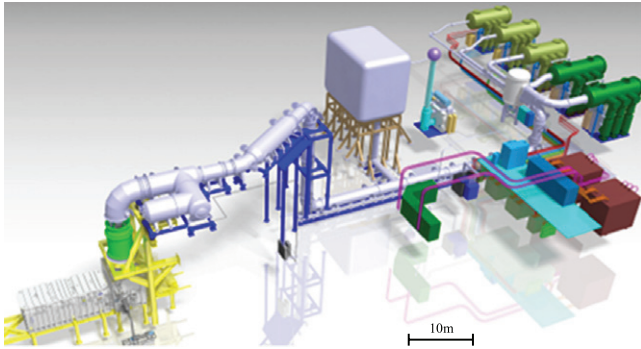


**Figure 3.** Overall view of the MITICA power supply including transmission line.

and between each pair of panels a dc voltage of up to 20kV is applied, plus, if necessary, an alternating voltage with a trapezoidal waveform of up to  $\pm 5$  kV can be applied. The alternating voltage will sweep the deflected beams along the panels, reducing the average peak power density on the panels. The E-RID is designed to absorb and remove a total power of about 19 MW and to withstand power densities of up to  $8 \text{ MW m}^{-2}$ . Given the high heat loads applied to this component and the resulting thermal stresses, the panels are made of CuCrZr alloy. The calorimeter consists of two panels in V configuration, whose aim is to absorb the energy of the beam, up to 18 MW. Two large cryo-pumps will also be installed on either longitudinal side of the BLV. Each cryo-pump has an overall surface of  $8 \times 2.6 \text{ m}$  and features a cryogenic circuit at  $\approx 5.5 \text{ K}$  (average temperature) cooling cryosorption panels, surrounded by thermal shields kept at  $\approx 80 \text{ K}$ . The cryo-pumps will be able to ensure a pumping capacity of  $4700 \text{ m}^3 \text{ s}^{-1}$  in  $\text{H}_2$ . The conceptual scheme of the MITICA power supplies was developed with the main aim to improve the feasibility of the scheme with respect to the ITER 2001 design [21] and in particular of the implementation of the RF driven ion source and the accessibility to the power supply devices in the future operation in ITER [22].

Output power of MITICA AGPS (Acceleration Grid Power supply) and ISEPS (Ion Source and Extractor Power Supply) is transmitted to the injector via a 1 MV transmission line (TL) [23, 24], longer than 100 m. It consists of a metal tube containing all active conductors and insulated by high-pressure  $\text{SF}_6$  gas (nominal pressure of 6 bar at  $20^\circ \text{C}$ ). In the last part, the TL also hosts the pipes carrying cooling water to the acceleration grids and to the ion source. The TL is connected to the vessel through a HV bushing [25] which also acts as a barrier between the pressurized gas contained in the TL and the vacuum environment in the vessel. It is designed to provide a double barrier, a fundamental requirement in nuclear power plants such as ITER. MITICA ISEPS is a set of power supplies feeding the ion source, including four 1 MHz RF generators rated at 200 kW [26]. The ISEPS is contained in a Faraday cage, named HVD1 [27], insulated from ground for up to  $-1 \text{ MV}$  and supplied through a  $-1 \text{ MV}$  insulating transformer. The external size of the HVD1 is  $12 \times 8 \times 10 \text{ m}$  (L  $\times$  W  $\times$  H). The HVD1 will be housed inside a HV hall of appropriate dimensions ( $26 \times 29 \times 21.5 \text{ m}$  internal size) to ensure the insulation and will be connected to the TL via

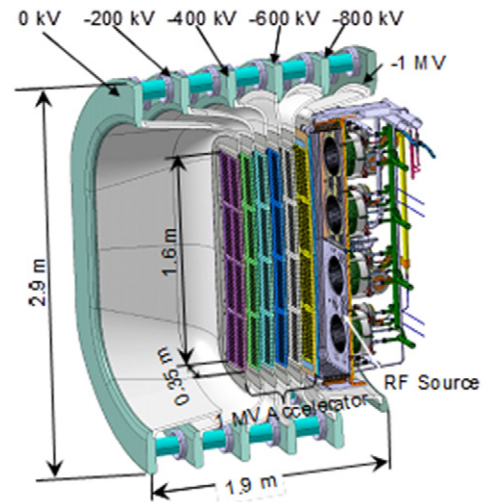


**Figure 4.** MITICA beam source.

an air/gas bushing placed below the HVD1. The HV hall will host also the  $-1 \text{ MV}$  insulating transformer and will be crossed by the transmission line installed inside a pit. MITICA AGPS [28] will apply voltage to the acceleration grids, 200 kV across each pair of adjacent grids for a total of 1 MV. AGPS is based on five 200 kV units, each consisting of one inverter generating three-phase 150 Hz square wave voltages, a step-up insulating transformer, a rectifier diode bridge and a RC filter. The output stages are connected in series to produce a voltage up to the nominal value of 1 MV. Finally, there are two further plant systems dedicated to MITICA: a) a cryogenic plant [29] capable of feeding the cryosorption panels with supercritical helium at 4.6 K and the thermal shields with gaseous helium at  $\approx 80 \text{ K}$ . The system is sized to remove, under pulse-on mode, up to 800 W through the supercritical helium circuits and 17 kW through the gaseous helium circuits. Further specific requirements come from the needs for 100 K regeneration of cryopumps between two consecutive long pulses or between trains of short pulses, when the cryosorption panels are saturated with  $\text{H}_2$ . b) A gas storage and handling plant needed to load and unload the  $\text{SF}_6$  gas from the HV gas insulated components. It is able to handle and store the  $\text{SF}_6$  gas necessary to insulate all HV components, i.e. TL's, diode rectifiers, filters, etc. The total quantity of  $\text{SF}_6$  gas is in the order of 30 tons.

### 2.3. SPIDER

SPIDER is the prototype of the negative ion source for ITER heating and current drive NBI. The source design, of the RF type, is based on the R and D carried out at IPP during the past years, with additional improvements to achieve long duration pulses (up to 1 h) on a full ITER-size ion source, in a full vacuum environment and with optimized beamlet optics. The SPIDER BS is designed to accelerate the beam up to 100 kV with a total beam power of 6 MW. It includes 8 RF antennas and an expansion chamber to produce the plasma from which ions are extracted and a set of grids for the extraction and acceleration of the negative ion beam. Each grid of

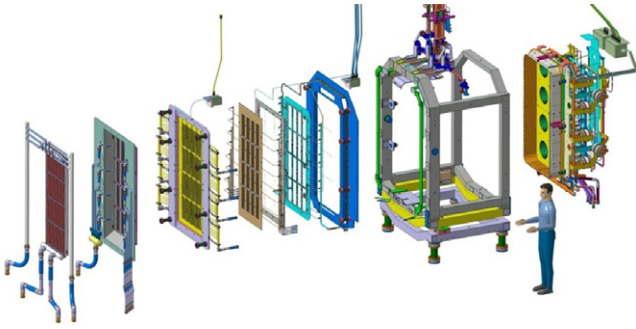


**Figure 5.** Exploded view of the SPIDER beam source.

about  $2\text{ m}^2$  is provided with  $4 \times 4$  groups of  $16 \times 5$  apertures for a total of 1280 openings having the same geometry as for MITICA and the ITER NBI system. A magnetic field designed to increase the current density of extracted negative ions, is produced by a current of some kA flowing in the grid facing the ion source plasma. Extraction grid and grounded grid are equipped with a carefully designed combination of permanent magnets and ferromagnetic materials [30] in order to suppress the co-extracted electrons, while compensating in a novel way for the corresponding distortion induced on the ion trajectories [31]. The grids and the main components are actively cooled [32]. SPIDER is also provided with an original electron dump, just outside the accelerator, made of several vertical pipes suitably arranged so as to absorb most of the power associated to electrons exiting the accelerator and mainly generated in it by stripping reactions [33], RF matching network components and vacuum capacitors are installed on the rear side of the ion source [34]. An exploded view of the SPIDER beam source is shown in figure 5; details about the progress of its procurement are reported in [13, 35].

SPIDER will have two calorimeters: the water-cooled beam dump (see figure 6) [36], which allows to absorb and remove the maximum power of 6 MW for a duration of up to 1 h, is instrumented with thermocouples to study the power balance and the beam uniformity at relatively low resolution. A high-spatial-resolution (2 mm), uncooled calorimeter (STRIKE) [37] will only be used for pulses of a few seconds duration ( $<10\text{ s}$ ). The source and the two calorimeters will be housed inside an AISI 304L cylindrical vacuum vessel [38] about 6 m long and 4 m in diameter. The vessel is composed of two cylindrical modules and two torispherical lids at the ends (see figure 7). A large number of ports are located on modules and lids to allow access for diagnostics purposes and connection to service lines.

SPIDER power supplies (PS) include two systems: the AGPS and the ISEPS. SPIDER ISEPS is identical to MITICA ISEPS. ISEPS is hosted inside a metallic cage, named HV deck (HVD) insulated with respect to ground to 100 kV and fed by an insulating transformer. The HVD is connected to the vessel by an air insulated transmission line (TL). AGPS [39] is a power supply rated for 96 kV / 71 A. It is based on pulse step modulation technology [40] that includes three oil insulated multi-secondary transformers and 150 switching modules. The HVD [41], operating as a Faraday cage, has an internal surface of about  $12 \times 11\text{ m}$ .

Figure 8 shows an overall view of the SPIDER PS. SPIDER will be equipped with a control system (CODAS) [42], a protection system (interlocks) [43] and with a complete set of diagnostics [44]. Diagnostics are essential in MITICA to qualify and optimize the NBI for ITER and to assess the amount of information on the source and beam that cannot be gathered by means of the reduced set of diagnostics, mainly thermocouples, available on the ITER NBI. In particular the objectives are to characterize the beam intensity profile and divergence with a set of complementary diagnostics and the source extraction region measuring the negative ion density and the caesium dynamics, to correlate the physics of the source with the beam characteristics, to verify the design and to investigate the operational space of beam source and injector.

### 3. Status of the MITICA and SPIDER projects and general plan

Buildings, auxiliary plants and medium voltage distribution system supply grids are directly funded by the Italian government whereas all the experimental equipment including cooling, cryogenic and vacuum and gas injection plant systems, owned by ITER, will be procured in kind by the Domestic Agencies that are involved in the project, F4E, JADA and INDA, as stated in the ITER agreement. SPIDER is realized with the contribution of F4E and INDA: INDA provides the beam dump and AGPS, F4E everything else including cooling and vacuum and gas injection systems.

MITICA is realized with the contribution of F4E and JADA: JADA provides the AGPS HV components (step-up transformers, diode rectifiers, filters, etc), the TL, the  $-1\text{ MV}$  insulating transformer and the HV bushing; F4E provides all the other MITICA components and plant systems.

The building construction started in October 2012. Completion is expected by the beginning of 2015, including all the building services. The common plant systems (cooling and GVS plants) are under procurement and their installation started in autumn 2014 with the equipment necessary for the SPIDER experiment. Completion of the common plant systems is foreseen by the end of 2015.

The final design and technical specifications for the supply of SPIDER components have been completed and all the procurement contracts have been assigned and the supplies are in progress. In particular, at the beginning of 2015 the installation is expected to start with HV Deck and vacuum vessel and to be completed within 2015 with the beam dump, the other PS systems including the TL, CODAS and interlocks. After completion of the PS installation, the commissioning of common plant systems and PS on dummy loads will be performed. Finally, in spring 2016, the beam source will be installed and, after the integrated commissioning, the SPIDER experimental phase will start.

The design phase of the MITICA BS and BLCs was completed by the end of 2014 and the final design review phase will be completed in the first months of 2015. In the meantime, some contracts for the procurement of the vessel and of



**Figure 6.** SPIDER vacuum vessel during assembly at supplier premises for factory tests.

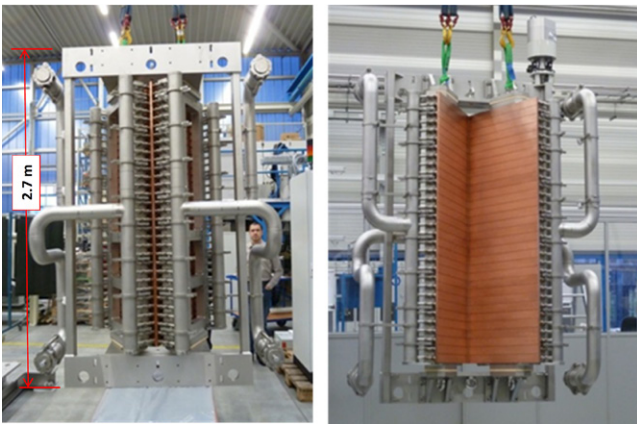


**Figure 7.** SPIDER water cooled beam dump.

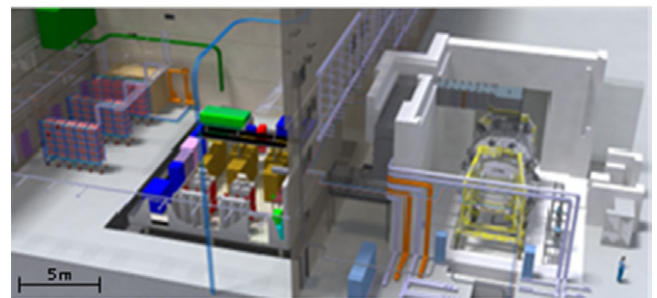


**Figure 8.** Overall view of the SPIDER power supply including vessel and transmission line.

the various PS systems are either already assigned or under call for tender. By 2015 all the tenders will be launched and most contracts placed. All JADA contracts were awarded and the supplies are currently under manufacturing by Japanese firms. The installation phase of the first components, i.e. TL and HV PS components will start in December 2015 and will continue until spring 2017. This phase will be followed by the integrated commissioning of all plant systems with CODAS and interlocks and by the PS integrated tests. After the installation of the MITICA BS and BLCs, the final integrated commissioning will follow and then the first experimental phase will start.

#### 4. Issues and solutions for improvements

Some of the ingredients which make unique the realization of these projects are the dc HV and high power conditions, the physics and engineering issues linked to the beam generation and some specific technological problems due to very heavy thermo-mechanical and electrical working conditions. So challenging requirements call for continuous studies in all the phases of the realization, from the conceptual design to the future operation.

In particular, the finalization of the design of the MITICA injector required considerable developments to tackle issues that could not be fully solved during the conceptual design phase [46–49]. Here in after are described and discussed the most significant studies and solutions worked out to complete the design of the MITICA beam source, to solve the HV holding issues in vacuum and to address the main technological challenges for the manufacturing of MITICA and SPIDER in-vessel components.

##### 4.1. MITICA beam source optimization

The physics and engineering design of MITICA beam source has considerably evolved during the last years with respect to the original multi aperture multi gap (MAMuG) design solution of the ITER HNB [1, 2, 10]. Several improvements have been conceived for the solution of critical issues in the design of the negative ion source and of the accelerator, which emerged in the course of the detailed analyses or in relation to the most recent results obtained from experimental devices at IPP and JAEA. Moreover, the stringent requirements concerning the beam optics (overall beam divergence  $<7$  mrad) and the limits imposed by thermo-mechanical, hydraulic, electrical and gas pressure constraints required an integrated and iterative design process. This design evolution involved the introduction of several new concepts [50], supported by new, specifically developed simulation codes, as well as by available experimental results.

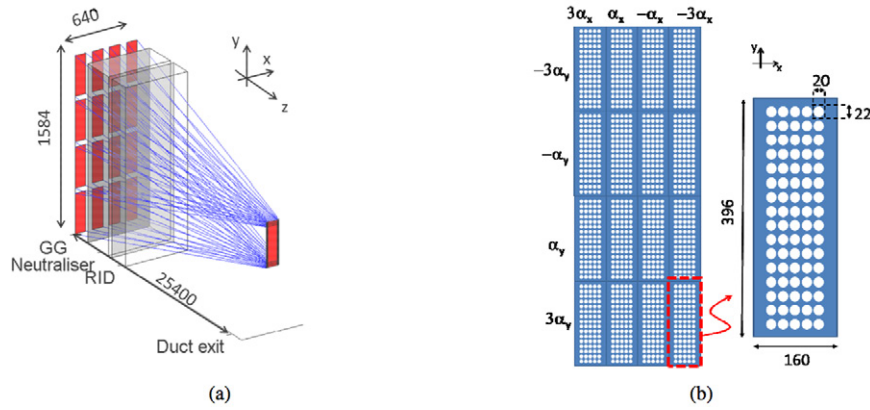


**Figure 9.** General scheme of the MITICA beam focusing (a), and detail view of an acceleration grid, constituted by  $4 \times 4$  beam groups (b). The aiming angles for each beam group in the grid are also shown. Sizes are in mm.

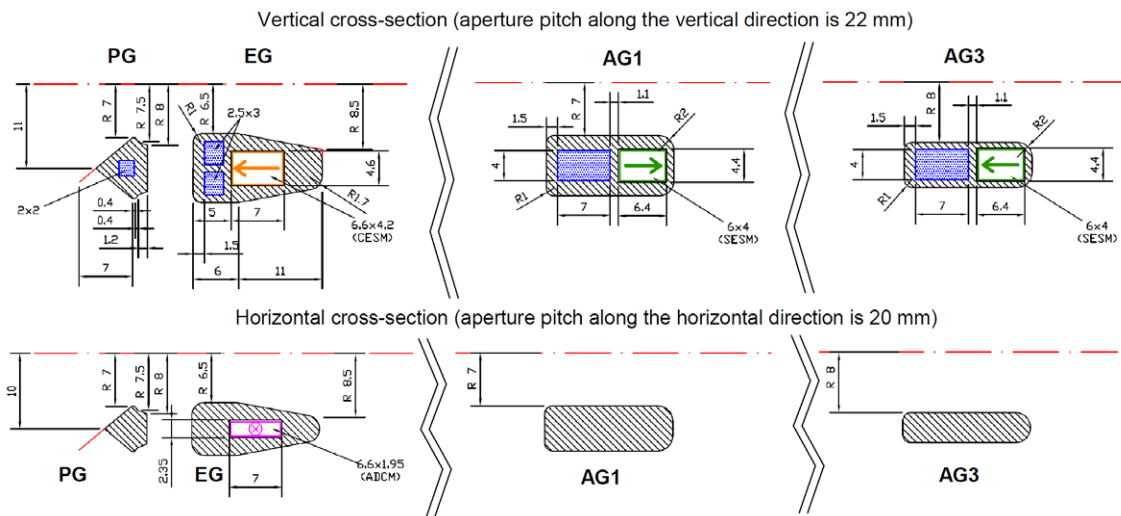


**Figure 10.** Cross section of the MITICA acceleration grids. The AG2 is identical to AG1 and AG4 is identical to AG3. The GG is also identical to AG3, but has no magnets. Aperture diameter is 14 mm for PG, EG, AG1 and AG2, and 16 mm for AG3, AG4 and GG.

Particularly innovative solutions were introduced in the beam source design in the following fields:

- Reduction of heat load on the accelerator grids (figures 9 and 10) by optimized disposal of co-accelerated electrons: a new magnetic field configuration in the multi-stage accelerator was developed, which deflects the co-extracted electrons and the electrons generated by stripping reactions as soon as possible. The new configuration (figure 11) is produced by a combination of a ‘local vertical field’ produced by permanent magnets embedded in the extraction grid (EG) and the acceleration grids (AG1–AG4) and of a ‘long-range horizontal field’ produced by a current flowing in the plasma grid (PG) and in the related busbars [51].
- Reduction of heat load on the accelerator grids by reduction of stripping reactions related to background gas pressure. More precise gas dynamics simulations led the modification in the mechanical design of the accelerator grid supports, so as to increase pumping efficiency and reduce the frequency of stripping reactions [58].
- Optimization of the magnetic ‘filter field’ configuration on the upstream side of the PG to improve the negative ion production (total current up to 40A). A completely new concept [65] for the PG busbars was developed, which guarantees the required field strength and uniformity, with reduced stray field in the RF drivers (figure 11), which was suggested by operational experience on the RF-driven ion sources at IPP [53].
- Improvement of grid cooling capability. An optimized cooling water distribution and a new design of cooling channels were introduced. Due to the very limited space available inside the acceleration grids and the very high heat loads, the new approach called nozzle island cooling enhancement (NICE) for the cooling channels was adopted [54, 55] for increasing the heat-exchange surface and water turbulence on the most loaded grids (AG1, AG2, AG3, AG4 and GG).
- Reduction of thermo-mechanical stress of the accelerator grids: a modified grid design with sliding mechanical supports and stress-relieve slits was adopted to ensure

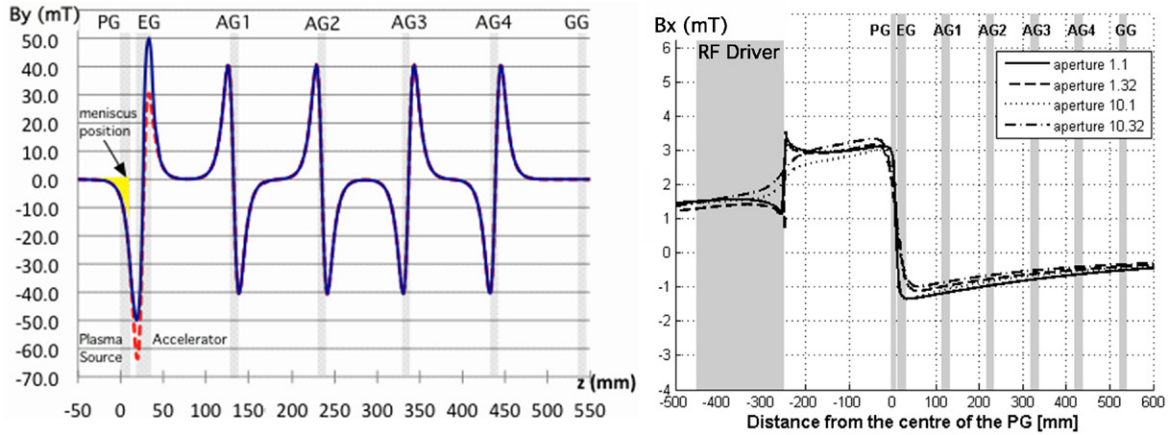


**Figure 11.** Profiles of the vertical ( $B_y$ ) and horizontal ( $B_x$ ) components of the transverse magnetic field in the ion source and in the accelerator after the optimization.

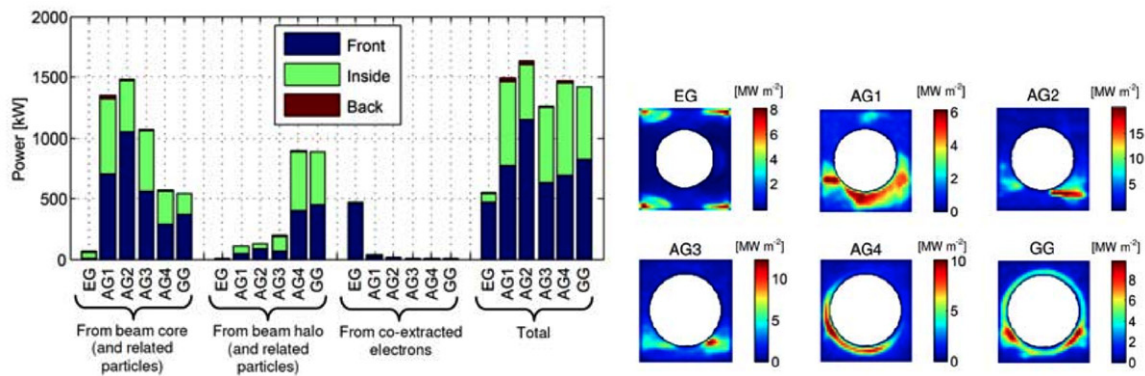


**Figure 12.** Transmitted and deposited heat loads on the MITICA grids (a), distribution of deposited power density ( $\text{MW m}^{-2}$ ) on the upstream surface of each grid (b).

free thermal expansion within each grid segment and to guarantee the required fatigue life for the grids.

- f) Correction of undesired beamlet deflections: progress of the detailed mechanical design of the accelerator showed that some solutions originally proposed were hardly applicable and stimulated different solutions for the correction of beamlet deflections of various origin and for beamlet aiming. In particular a new layout of the extraction grid magnets has been developed and patented. This guarantees the ‘intrinsic’ cancellation of the magnetic zig-zag deflection caused by the electron-suppression magnets in the extraction grid [52]. The correction of the deflections due to beamlet-beamlet repulsion will rely on metallic steering plates (kerbs) attached to the grids on the downstream face at both sides of each beam group. Improvement and simplification of beamlet aiming was also achieved, based on geometrical orientation of each beam group (figure 9).
- g) In consideration of the uncertainty margin still existing on the best configuration for  $\text{H}^-$  and  $\text{D}^-$  ion extraction and electron suppression in a 1 MV accelerator, the possibility of adjusting the magnetic field profile for a rapid experimental validation of the beam injector has also been considered, in accordance with the main scientific objective of MITICA [65].

The combination of the above described improvements will produce a substantial reduction of the heat load on the grids (figure 12), which are expected to remain below the acceptable limits for long-pulse operation (3600 s) and fatigue life of the grids (50 000 beam on/off cycles).

#### 4.2. HV holding in vacuum

The voltage holding in the ITER and MITICA beam source is recognized to be one of the most critical issues. In fact, the complex extraction and acceleration systems, formed by electrodes polarized at different potentials immersed in vacuum or in a low-pressure gas, shall operate for a very long pulse duration (3600 s) at high current (40 A).

The operating conditions of pressure ( $p$ ) and typical dimensions ( $d$ ) of the system correspond to the region on the left-hand side of the Paschen curve ( $p \cdot d < 0.1 \text{ Pa} \cdot \text{m}$ ), where the breakdown is no longer determined by the classical—well predictable—Townsend discharge, but it is determined, for the long-gap case, by a complex phenomenology, far from being well understood, in which different breakdown mechanisms (e.g. Slivkov–Cranberg Clump Theory and the Latham Photoelectric Cascade Mechanism) are likely concurrent.

To solve the design issue of the optimization of the electrode profiles for such a complex multielectrode—multivoltage

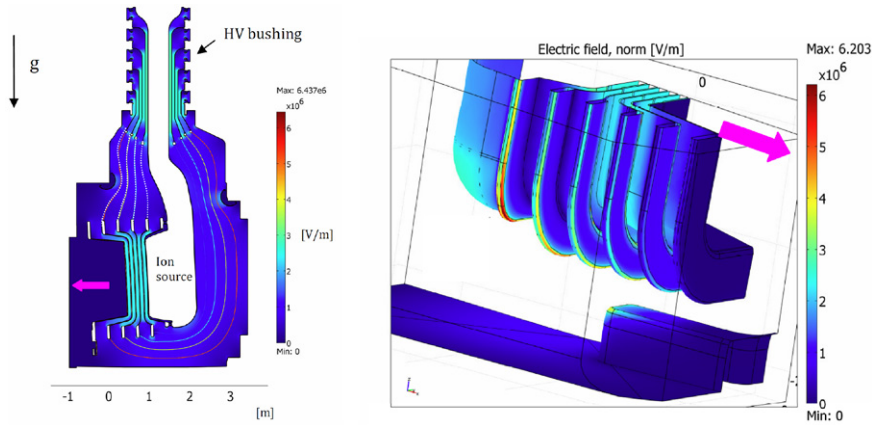


**Figure 13.** Electrostatic field maps in vertical middle plane and in the bottom region of MITICA beam source.

electrostatic configuration, a R and D activity was carried out on the basis of the experiments performed at the JAEA Megavolt Test Facility [59], at the HVPTF [45] and of those reported in literature. The result of this work was the development of an innovative voltage breakdown predictive model, capable to identify, for any electrostatic configuration, the breakdown probability for a given applied voltage [60, 61].

This model was applied (see figure 13) to optimise the electrostatic shape of MITICA beam source screen, the accelerating grids screens and the vacuum vessel.

The simulated breakdown voltage distributions so far obtained for MITICA beam source in high vacuum conditions [60] show anyhow the criticality of voltage holding above 600 kV, but this does not yet take into account the improvement of performance which can be obtained by exploiting the ‘pressure effect’ described in [62], when raising the background gas pressure up to  $10^{-4}$ – $10^{-3}$  mbar.

Further improvements in the voltage holding are expected to be gained by optimizing the voltage conditioning procedure; to this purpose, experiments have been done [61] and are in progress.

Additionally the presence of magnetic field affects voltage holding. This effect, in the operating pressure range of MITICA, produces an increase of the trajectory length of any charged particle, thus modifying the Paschen product  $p \cdot d$ . Experiments have been carried out at the HVPTF, and the results have been successfully interpreted by numerical simulations. A deviation towards the lower pressure region of the left branch of the  $H_2$  Paschen curve due to magnetic field has been observed and properly modelled. However, according to the results obtained [63], this effect could be overcome by applying the external magnetic field after the full voltage has been reached.

#### 4.3. Technological issues

Several challenging technological issues for manufacturing of in-vessel components were to be addressed. The latest and most significant ones are presented in the following sections, highlighting the provisions adopted to face and solve them.

**4.3.1. Alumina post insulators.** The pure alumina insulators for SPIDER and MITICA beam sources are critical components requiring accurate design and verifications, prototyping and dedicated qualification tests before production [57].

The MITICA post-insulators are shown in figure 4: each 200 kV voltage step is held by 18 cylindrical insulators put in parallel. Each insulator, see figure 14(a), is made of high purity alumina grade C799. Stainless steel flanges are fixed to the alumina cylinder by means of screws directly tightened on threaded holes in alumina 16.

The post-insulators are subjected to relatively high forces induced by the weight ( $\sim 20$ t) and seismic loads acting on the whole beam source.

The most demanding load configuration for the post insulators was identified and adopted for qualification by mechanical tests. The load scheme and the corresponding test equipment are shown in figure 14.

The SPIDER alumina insulators, holding a maximum test voltage of 140 kV, are similar to the MITICA ones, with slightly reduced dimensions (max diameter 110 mm), given the much lower forces applied.

Several mechanical and electrical tests were carried out both on SPIDER and MITICA insulators prototypes and the results show that manufacturing of insulators having such dimensions requires a careful choice of alumina base material and an optimized and well controlled sintering process, since differential shrinking of peripheral and core volume can generate large residual stresses in the bulk material.

The SPIDER insulators were successfully manufactured with alumina grade C795 ( $Al_2O_3$  96%) having a higher content of glassy phase and a properly optimized sintering process. The electrical tests on all the ceramic insulators were passed applying 140 kVdc for more than 3 h without any breakdown. Compression tests on the insulator between beam source and vacuum vessel were passed with a compression load greater than 100 kN without any structural damage to the ceramic insulator. The insulators prototypes between grounded grid and extractor and between beam source and extractor were tested by specific bending and shear proof tests. In both cases the mechanical tests were passed successfully.

The MITICA insulators based on the original solid cylindrical design achieved the required electrical performances,

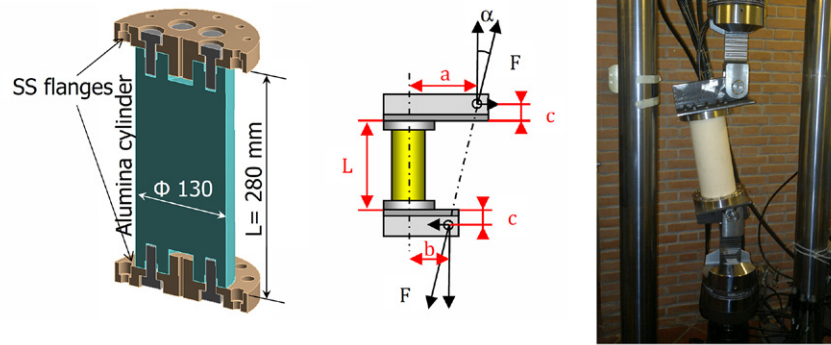


**Figure 14.** (a) Cross section view of a typical 200kV alumina post-insulator; (b) scheme of testing load condition for MITICA BS post-insulators ( $F = 53 \text{ kN}$ ,  $\alpha = 10.51^\circ$ ,  $a = 118 \text{ mm}$   $b = 34.5 \text{ mm}$   $c = 60 \text{ mm}$ ) and (c) corresponding test equipment.

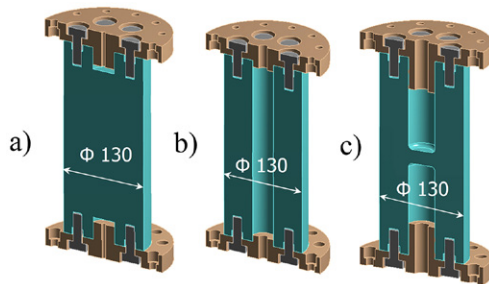


**Figure 15.** Alternative geometries for MITICA 200kV post-insulators: (a) solid insulator, (b) hollow insulator, (c) 'H' section insulator with metalized blind holes.

but demonstrated a limited mechanical strength, due to lack of homogeneity in alumina and residual thermal stresses. Alternative design solutions such as hollow cylinders (b) and (c) in figure 15 have been considered, with the possible insertion of a Vespel<sup>R</sup> insulating rod to enhance the HV holding in case (b).

The mechanical tests on configuration (b) have shown good mechanical behaviour, but reduced voltage holding capability, due to the occurrence of micro discharges and relevant gas release inside the relatively small volume (0.27 l).

The configuration (c) has revealed some issues during sinterization in case of high purity alumina (C799). The same geometry (configuration c) made by less pure alumina (C795) can be manufactured but its mechanical behaviour does not fulfil the mechanical requirements yet.

The electrical tests were finally passed for solution (b) inserting a special rod made by Vespel<sup>R</sup>. The rod was inserted inside the insulator hollow with a radial interference of 0.03 mm in diameter exploiting the difference in thermal expansion coefficient between alumina and Vespel<sup>R</sup>. The rod was cooled up to  $-20^\circ\text{C}$  before assembly. A voltage up to 250 kVdc was hold in high vacuum without any breakdown. The insulator type (b) with the Vespel<sup>R</sup> rod is the reference solution for MITICA Beam Source, being the sole configuration which has passed both electrical and mechanical tests.

**4.3.2. Thick molybdenum coating of beam source components.** A thick Mo coating (about 1 mm) is required on the copper back-plate of MITICA ion source to limit sputtering

effects due to focused back-streaming ions. A specific explosion bonding process was developed and optimized on some prototypes.

The power density due to back-streaming ions is highly peaked, achieving up to  $60 \text{ MW m}^{-2}$  on areas of about  $3 \text{ mm}^2$ . Since local stresses are then induced by the differential thermal expansions of bonded layers (Cu and Mo) detailed thermo-mechanical analyses have been performed to assess the design reliability. Some preliminary thermal proof tests demonstrated the robustness of the identified solution [56]. Small scale prototypes reproducing the actual back-plate structure and water cooling configuration have been then prepared (see figure 16), for final qualification thermal tests on the GLADIS facility (up to  $26 \text{ MW m}^{-2}$ ). These tests have been recently carried out: more than 100 beam pulses were performed with maximum power density up to  $20 \text{ MW m}^{-2}$ , for a total exposure time of about 1000 s. The surface temperature of molybdenum has been continuously measured and recorded by means of two pyrometers during the pulses and never exceeded  $650^\circ\text{C}$ . Moreover the maximum temperature remained stable from the first to the last pulses, showing that no evident progressing damage was affecting the test samples. Further six thermocouples were also inserted in the copper substrate to monitor its temperature. The heat power applied during each pulse at regime was of about 215 kW, causing a temperature increase of the  $1 \text{ kg s}^{-1}$  cooling water of about  $50^\circ\text{C}$ . In figure 17 a view of the prototypes installed in the GLADIS facility and a picture taken from the infrared camera during a pulse are shown.

The tests have been successfully concluded, since no damage have been found during the test campaign, nor after, during the visual inspection of the samples.

These successful results, demonstrated the reliability of Mo–Cu interface obtained by explosion bonding for the MITICA Beam Source.

**4.3.3. Beam source manufacturing.** Both SPIDER and MITICA beam sources require specific technological developments to fulfil very tight tolerances on misalignments among the correspondent apertures of extraction and acceleration grids. Keeping the relative positions of 1280 apertures within  $\pm 0.2 \text{ mm}$  on grids having overall dimensions of  $0.8 \times 1.8 \text{ m}$  is actually at the limit of available tools and

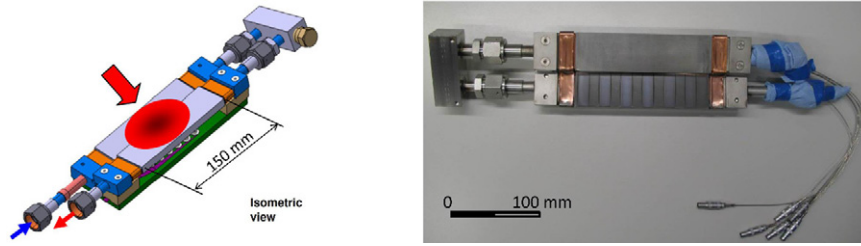


Figure 16. Prototypes for thermo-mechanical tests of Mo coated Cu samples.

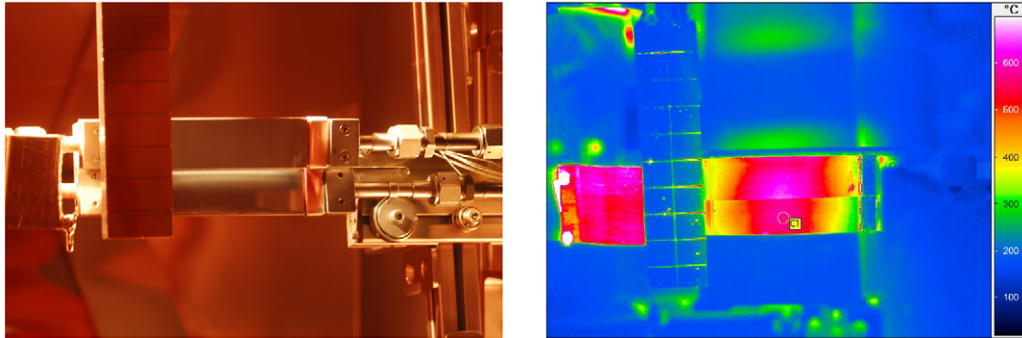


Figure 17. Views of the prototypes installed in GLADIS facility (left) and infrared camera measurements during one pulse (right).

processes. Subdividing the large grids in four horizontal segments having smaller dimensions makes possible the very precise drilling of apertures with maximum errors of  $\pm 0.02$  mm with respect to reference holes for each segment. A first segment of the grounded grid machined for SPIDER beam source is shown in figure 18. Positioning and fixing of each segment is then guaranteed by dowel holes precisely machined on supporting frames.

An accurate assembly process with several intermediate positioning controls and adjustments using laser tracker instruments is being specifically developed by the beam source suppliers to adjust the absolute positions of the grids. The experience and results obtained on SPIDER beam source will be also significant for the most critical procurement of the MITICA Beam Source.

**4.3.4. Beamline components.** The core parts of MITICA beam line components are relatively thin (22–40 mm) panels made of OF copper or CuCrZr alloy, actively cooled by water flowing inside circular channels with twisted tape for enhanced heat exchange performances. The water flow rate in the beam line components has been determined on the basis of the deposited beam power and the maximum water temperature:  $55 \text{ kg s}^{-1}$  to exhaust the 6 MW expected at the Neutraliser,  $100 \text{ kg s}^{-1}$  for the 18 MW at the E-RID, and  $100 \text{ kg s}^{-1}$  for the 18 MW at the Calorimeter. The flow rate was verified by mono-dimensional and computational fluid dynamics (CFD) analyses considering the flow behaviour in the complex local geometries. The flow temperature distribution in convective conditions and overall out of plane deformations of the middle panels are shown in figure 19.

Some R and D activities have been carried out for the 2 m long cooling channels manufactured by deep drilling and by insertion of 2 ÷ 4 mm thick twisted tapes as represented in figure 20. An out of axis drill deviation of 1 mm has been

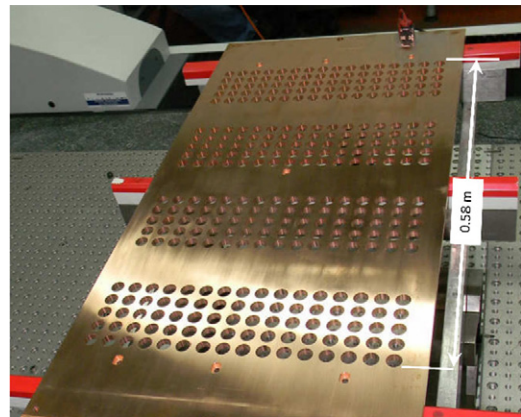
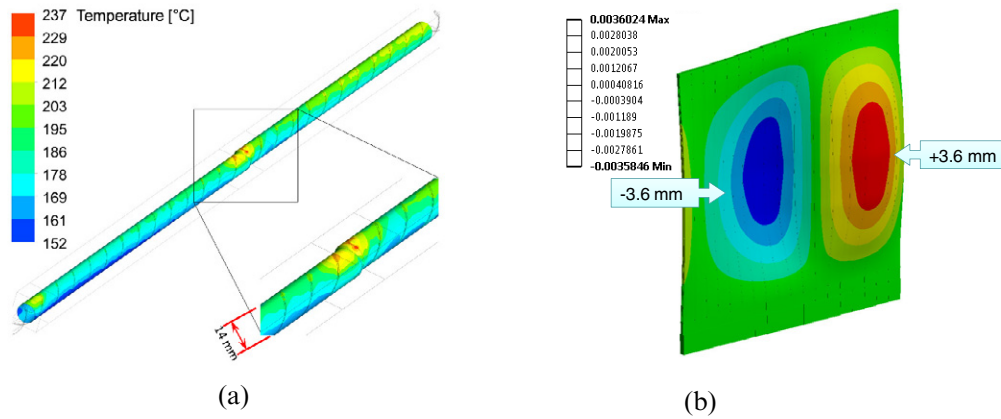


Figure 18. The first segment of grounded grid manufactured for SPIDER.

achieved on 1 m long and 14 mm diameter holes in CuCrZr panels. Double-side drilling has been judged feasible and local effects due to such errors have been verified by measuring the residual wall thicknesses after drilling using a multi-mode ultrasonic thickness gauge.

The high voltage panels (up to 25 kV) of the E-RID will be electrically insulated by two cooling breaks at the main cooling manifolds and by standoff insulators at the supporting structure. They will be produced by metal-ceramic joining of stainless steel TP 316L to polycrystalline alumina. Grade A1 low porosity alumina shall be used for the high purity level compatible with the radiation environment, having small average defect dimension with reduced variability in size (Weibull modulus  $m > 10$ ), negligible corrosion and creep below  $800^\circ\text{C}$  and limited susceptibility to slow thermal cycles.

Liquid state diffusion bonding was selected for the E-RID cooling breaks, being the most common method for manufacturing long term stable joints ensuring leak tightness ( $10^{-10}$



**Figure 19.** Thermo-mechanical analyses of the RID middle wall under beam-on thermal loads. (a) Flow temperature distribution in E-RID cooling channel with swirled tape. (b) Displacements [mm] of the E-RID middle wall under beam-on thermal loads.

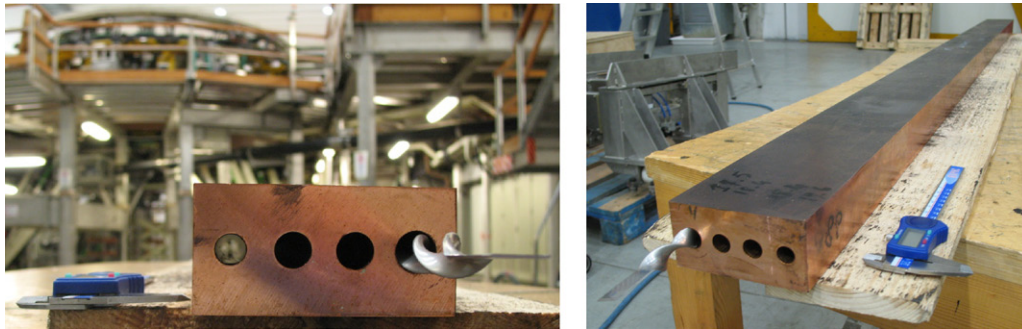


**Figure 20.** Drilled CuCrZr plate with inserted a turbulence promoter with 2 mm thickness.

$\text{Pa} \cdot \text{m}^3 \text{s}^{-1}$  helium leak rate) and high integrity joints with tensile strength around 100 MPa. In the metal to ceramic joint a foil of filler metal (Cusil™) will be used as a compliant interlayer to aid the bonding process and to limit post-bond thermal stresses [64].

## 5. Conclusions

Substantial progress in the realization of the PRIMA neutral beam test facility has been achieved. The building services are being completed and the common plant systems are expected to be ready by the end of 2015. All the SPIDER procurement contracts were awarded and the supplies are in progress following the plan according to which the integrated commissioning starts in 2016. The design phase of the MITICA BS and BLCs is being completed; in 2015 the tenders will be launched and most contracts placed. JADA contracts were awarded and the supplies are currently under manufacturing. The installation phase of the first components, i.e. TL and HV PS will start in December 2015 and will continue until 2017; the integrated commissioning and the first experimental phase will follow.

Critical issues were tackled to finalize the design of the MITICA injector and specific R and D tasks, requiring the development of new simulation codes and concepts, were launched to address them, with effective results. Some innovative solutions introduced in the MITICA beam source design allow reducing the heat load in the acceleration grids,

improving the grid cooling capability, reducing the thermo-mechanical stress and also correcting undesired beamlet deflection. An innovative voltage breakdown predictive model was developed and utilized to design the electrostatic shape of the MITICA beam source screen, accelerating grid screens and vacuum vessel. Finally, significant progress in the solution of some technological issues has been achieved.

## Disclaimer

The work leading to this publication has been funded partially by Fusion for Energy under the Contract F4E-RFX-PMS\_A-WP-2014. This publication reflects the views only of the author, and Fusion for Energy cannot be held responsible for any use which may be made of the information contained therein.

The views and opinions expressed herein do not necessarily reflect those of the ITER Organization.

## References

- [1] ITER Physics Basis Editors *et al* 1999 *Nucl. Fusion* **39** 2495
- [2] ITER Technical Basis 2002 section 5.3 DDD5.3-IAEA Vienna
- [3] Kraus W. *et al* 2010 *Rev. Sci. Instrum.* **81** 02B110
- [4] Kraus W. *et al* 2008 *Rev. Sci. Instrum.* **79** 02C108
- [5] Kojima A. *et al* 2010 *Rev. Sci. Instrum.* **81** 02B112
- [6] Takeiri Y. 2010 *Rev. Sci. Instrum.* **81** 02B114
- [7] Taniguchi M. *et al* 2010 *Rev. Sci. Instrum.* **81** 02B101

- [8] Bonicelli T. et al 2006 *ITER2-3Rd Proc. 21st IAEA Conf. (Chengdu, 16–21 October 2006)* (<http://www-pub.iaea.org/MTCD/meetings/Announcements.asp?ConfID=149>)
- [9] Jacquinet J. et al 2009 *Fusion Eng. Des.* **84** 125
- [10] Hemsworth R.S. et al 2008 *Rev. Sci. Instrum.* **79** 02C109
- [11] Sonato P. et al 2012 *Proc. 24th IAEA Fus. En. Conf. (IAEA, San Diego, USA, 8–13 October 2012)* ITR/1–3 <http://www-pub.iaea.org/iaea-meetings/41985/24th-Fusion-Energy-Conference>
- [12] Sonato P. et al 2013 *AIP Conf. Proc.* **1515** 549
- [13] Sonato P. et al 2009 *Fusion Eng. Des.* **84** 269
- [14] Speth E. et al 2006 *Nucl. Fusion* **46** S220
- [15] Fantz U. et al 2014 *Rev. Sci. Instrum.* **85** 02B305
- [16] Masiello A. et al 2014 *Proc. 25th IAEA Fus. Energy Conf. (Saint Petersburg, Russia, 13–18 October 2014)* <http://www-pub.iaea.org/iaea-meetings/46091/25th-Fusion-Energy-Conference-FEC-2014>
- [17] Fellin F. et al 2014 *Presented at the 28th SOFT 2014, (S. Sebastián, Spain)* (<http://www.soft2014.eu/welcome.html>)
- [18] Zaccaria P. et al 2012 *Rev. Sci. Instrum.* **83** 02B108
- [19] Dalla Palma M. et al 2015 *Fusion Eng. Des.* in press
- [20] Dalla Palma M. et al 2013 *Fusion Eng. Des.* **88** 1020
- [21] ITER Des. 2001 Descr. Doc. 4.1, Pulsed Power Supplies, ref. N41 DDD 16 01-07-06 R 0.3
- [22] Gaio E. et al 2008 *Fusion Eng. Des.* **83** 21–9
- [23] Watanabe K. et al 2006 *Nucl. Fusion* **46** S332–9
- [24] Watanabe K. et al 2009 *Nucl. Fusion* **49** 055022
- [25] Tobar H. et al 2010 *J. Plasma Fusion Res. SERIES* **9** 152–6
- [26] Bigi M. et al 2015 *Fusion Eng. Des.* in press
- [27] Boldrin M. et al 2013 *Fusion Eng. Des.* **88** 985–9
- [28] Toigo V. et al 2013 *Fusion Eng. Des.* **88** 956–9
- [29] Valente M. et al 2012 *12th Cryogenics 2012 IIR Int. Conf. (Dresden, Germany, 10–14 September 2012)* (<http://www.gasworld.com/12th-cryogenics-2012-iir-international-conference/48.event>)
- [30] Marconato N. et al 2011 *Fusion Eng. Des.* **86** 925
- [31] Agostinetti P. et al 2011 *Nucl. Fusion* **51** 063004
- [32] Marcuzzi D. et al 2009 *Fusion Eng. Des.* **84** 1253
- [33] Agostinetti P. et al 2012 *IEEE Trans. Plasma Sci.* **40** 629
- [34] Marcuzzi D. et al 2010 *Fusion Eng. Des.* **85** 1792
- [35] Pavei M. et al 2014 *Presented at the 28th SOFT 2014, (S. Sebastián, Spain)* (<http://www.soft2014.eu/welcome.html>)
- [36] Rotti C. et al 2013 *Proc. IEEE 25th Symp. of Fusion Eng. (San Francisco, CA, 10–14 June 2013)* (<http://sofe2013.org/index.php>)
- [37] Rizzolo A. et al 2010 *Fusion Eng. Des.* **85** 2268
- [38] Zaccaria P. et al 2015 *Fusion Eng. Des.* in press
- [39] Baruah U.K. et al 1997 *Proc. IEEE/NPSS 17th Symp. of Fusion Eng. (San Francisco, CA, 6–10 October 1997)* (<http://www-ferp.ucsd.edu/LIB/MEETINGS/9710-SOFE97/summaries.html>)
- [40] Förster W. and Alex J. 2002 *IEEE 25th Power Modulator Symposium (Hollywood, CA, 30 June–3 July 2002)* (<http://inspirehep.net/record/975403?ln=it>)
- [41] Boldrin M. et al 2015 *Fusion Eng. Des.* in press
- [42] Luchetta A. et al 2014 *Fusion Eng. Des.* **89** 663–8
- [43] Pomaro N. et al 2013 *Fusion Eng. Des.* **88** 980–4
- [44] Pasqualotto R. et al 2012 *Rev. Sci. Instrum.* **83** 02B103
- [45] De Lorenzi A. et al 2011 *Fusion Eng. Des.* **86** 742–5
- [46] Inoue T. et al 2001 *Fusion Eng. Des.* **56–57** 517–21
- [47] Hemsworth R. et al 2009 *Nucl. Fusion* **49** 045006
- [48] Grisham L.R. et al 2012 *Fusion Eng. Des.* **87** 11
- [49] De Esch H.P.L. et al 2013 *AIP Conf. Proc.* **1515** 512
- [50] Antoni V. et al 2014 *Rev. Sci. Instrum.* **85** 02B128
- [51] Chitarin G. et al 2013 *Fusion Eng. Des.* **88** 507
- [52] Chitarin G. et al 2014 *Rev. Sci. Instrum.* **85** 02b317
- [53] Franzen P. et al *Nucl. Fusion* submitted
- [54] Agostinetti P. et al 2015 Detailed design optimization of the MITICA negative ion accelerator in view of the ITER NBI *Nucl. Fusion* submitted
- [55] de Esch H.P.L. et al 2015 Physics Design of the HNB Accelerator for ITER *Nucl. Fusion* in press
- [56] Pilan N. et al 2015 *Fusion Eng. Des.* in press
- [57] Pavei M. et al 2013 *Proc. IEEE 25th Symp. of Fusion Eng. (San Francisco, CA, 10–14 June 2013)* (<http://sofe2013.org/index.php>)
- [58] Sartori E. et al 2014 *Rev. Sci. Instrum.* **85** 02B308
- [59] Kashiwagi M. et al 2015 *Fusion Eng. Des.* in press
- [60] Pilan N. et al 2011 *IEEE Trans. Dielectr. Electr. Insulation* **18** 553–60
- [61] De Lorenzi A. et al 2013 *IEEE Trans. Plasma Sci.* **41** 2128–34
- [62] Kashiwagi M. et al 2009 *Nucl. Fusion* **49** 065008
- [63] Pilan N. et al 2015 *IEEE Trans. Plasma Sci.* **42** 1012–20
- [64] DallaPalma M. et al 2015 *Fusion Eng. Des.* in press
- [65] Chitarin G. et al 2015 *AIP Conf. Proc.* **1655** 040008